Fast calculation method with foveated rendering for computer-generated holograms using an angle-changeable ray-tracing method

Lingjie Wei* and Yuji Sakamoto

Graduate School of Information Science and Technology, Hokkaido University, Kita 14, Nishi 9, Kita-ku, Sapporo, 060-0814, Japan
*Corresponding author: wlj@ist.hokudai.ac.jp

The computer-generated hologram (CGH) technique is a technique that simulates the recording of holography. Although the CGH technique has a lot of advantages, it also has some disadvantages; one of them is the long calculation time. Much research on the human eye has established that humans see 135° vertically and 160° horizontally, but can see fine detail within an only 5° central circle. Foveated rendering uses this characteristic of the human eye to reduce image resolution in the peripheral area and achieve a high calculation speed. In this paper, a new method for CGH fast calculation with foveated rendering using an angle-changeable ray-tracing method is introduced. The experiments demonstrate the effectiveness and high-speed calculation of this method.   © 2019 Optical Society of America

https://doi.org/10.1364/AO.58.00A258

1. INTRODUCTION

Recently, with the development of 3D technology, we have been requiring more realistic images and 3D experiences. Therefore, commercial products, such as 3DTV [1] and 3D game machines [2], have been developed along with conventional 2D display technology. 3D technology is quite common in our daily lives, and various studies have been conducted on it. 3D head-mounted display technology [3] is a technology that represents the future society as a display technology of "showing an object to be there." Although this technology easily generates vivid 3D objects, it may still make users feel impaired or sick, so a "natural" display method is hard to realize. However, holography has been proposed as the ultimate 3D display method that satisfies all of the physiological factors that humans require [4].

Holography is a technique for recording all light information to generate an interference pattern (hologram) by causing the interaction of coherent object light and reference light. The technique of using computer simulation to generate a hologram as electronic image data is called the CGH technique. This technique has some advantages, such as not needing a complicated optical system (which holography needs) and having the ability to generate animation. The CGHs in head-mounted displays are called holographic head-mounted displays [5]. However, they still have some problems, and one of these is the long calculation time.

We see 135° vertically and 160° horizontally, but we can see fine detail within an only 5° central circle. This tiny portion of the visual field in the retinal region is called the fovea [6]. Human eye acuity will fall off rapidly with increasing angular distance away from the central gaze direction due to the reducing receptor and ganglion density in the retina. In a 3D head-mounted display, the technology using this human eye characteristic to reduce the image resolution in the peripheral area and achieve a high calculation speed is called foveated rendering [7].

In this study, we propose a new method for CGH fast calculation with foveated rendering using an angle-changeable ray-tracing method. In this method, we can generate a CGH reconstruction image with a high calculation speed with greater freedom to control the size, position, and depth of the object. Also, with this method, we can adjust the resolution freely and realize resolution gradation in the case of aliasing of the reconstruction image. By using this method, we can generate a CGH reconstruction image with a higher calculation speed and with almost no observable effect for the viewer in a high-quality foveated rendering.

2. FOVEATED RENDERING

A. Foveated Rendering in Fast Calculation

Traditional computer-graphics (CG) rendering ignores the gaze direction of users and displays an image or an animation in very high resolution over the whole display. This is a huge waste of power and calculation resources. In traditional displays, the 5° central circle that the viewer gazes at fills only about 8% of the whole 60° screen; the situation is worse with head-mounted

displays because they have a much larger field of view. By tracking the user's eye gaze direction and showing an image with high resolution in the central area and low resolution in the peripheral area, we can omit ungazed at detail and render many fewer pixels and triangles than traditional CG rendering.

Some related work has used foveation with eye tracking hardware and foveated displays, and much previous work has been published. Some papers have covered eye tracking applications [8], eye tracking in 3D graphics [9], multi-resolution gaze-contingent display applications [10,11], and attention in display design [12]. Some papers have covered how degrading peripheral resolution affects visual search performance [13] and showed that peripheral resolution could be reduced by almost half without significantly degrading performance [14], which was examined using the effect of peripheral blurring at a high field of view (20°–30°), and it was found that contrast was a better indicator of search performance than size.

Our method resembles foveated rendering with image regions sampled at pixel distances of 1, 1/2, and 1/4 of native resolution. Because we expand the sampling interval, we can calculate fast by foveated rendering.

B. Acuity of Human Eye

Many works have shown how human eye acuity falls off in the peripheral area. Strasburger et al. [15] summarized the various strands of research on peripheral area vision and related them to theories of form perception. When measuring how a human eye's minimum angle of resolution would be changed based on increasing the angular distance away from the central gaze direction, we can get a result for the linear model, which is defined as

$$\alpha = me + \alpha_0, \tag{1}$$

where α is the minimum angle of resolution in degrees per cycle, e is the angular distance away from the central gaze direction, α_0 is the smallest resolvable angle and represents the visual acuity in the fovea region ($e = 0$, we choose the representative result in the minimum angle of resolution with the vision in 1.0, 0.017°), and m is the slope. This linear model shows the expected fall off of acuity with the angular distance changed when moving away from the central circle, where acuity is measured as the frequency of minimum angular resolution.

C. Conventional Method with Foveated Rendering for CGH

There is some previous research about applying the foveated rendering method to CGHs; one of these is about applying this in terms of hardware [16]. This method is mainly used for a 2D display with a CGH reconstruction image to realize the effect of foveated rendering. The 2D display is set at a depth of 1 m, which represents the peripheral area rendered in low resolution, and a CGH reconstruction image is set in the center of the whole scene, which represents the fovea region with high resolution. Therefore, in this method, only the center of the fovea region was displayed in the CGH; the other area was rendered only on the 2D display. Also, the depth of objects in the peripheral area was fixed to a certain extent. Another is about reducing the number of point lights in the peripheral area to realize fast

calculation [17], but this would cause the object in the peripheral area to become discrete points and would influence the viewers to observe the reconstruction image.

However, in our proposed method, we can generate a CGH reconstruction image with a fast calculation speed with more freedom to control the size, position, and depth of the object. Also, with this method, we can adjust the resolution freely and realize resolution gradation with almost no observable effect for the viewer.

3. PROPOSED METHOD

In this section, we will introduce our new method for CGH fast calculation with foveated rendering using an angle-changeable ray-tracing method. In this method, we can generate a resolution-adjustable CGH reconstruction image with a fast calculation speed that is suitable for the characteristics of the human eye and can control the size, position, and depth of the object freely without any change to the field of view. Furthermore, we did some experiments to show the correctness and high speed of our method with almost no observable effect for the viewer when he/she observes the reconstruction image.

A. Generating CGH

1. Point-Based Method

To generate CGHs, it is necessary to calculate the object light. There are some methods of calculating object light, which can be roughly divided into point-based methods [18], holographic stereogram methods [19,20], and Fourier transform methods [21].

In our proposed method, the object light is calculated by a point-based method, and then the CGH is generated using a ray-tracing method. The point-based method is a method of covering an object with many point light sources and calculating the object light. The advantage is that this method can be applied to any object by a lot of point light sources. However, as the number of point light sources increases, a longer calculation time is required.

When the point-based method is being used to display an object, the amplitude distribution on the hologram plane is indicated as shown in Fig. 1. Assuming that the position of a one-point light source is in P, the light wave from this point light source to the hologram plane H_i is represented by

$$H_i(x, y, z = 0) = \frac{A_i}{d_i} \exp(-jkd_i) \tag{2}$$

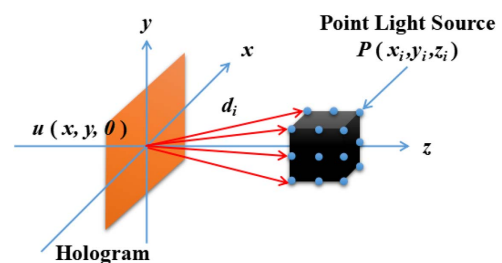The distance from the point source to the hologram plane is d_i:

Fig. 1.   Point-based method.

$$d_i = \sqrt{(x - x_i)^2 + (y - y_i)^2 + (z - z_i)^2} \quad (3)$$

A_i is the amplitude, k is $2\pi/\lambda$, and λ is the wavelength. Therefore, if the number of point light sources is N, the whole amplitude distribution on the hologram plane of the entire object to be displayed can be calculated by adding light waves from the respective point light sources by using Eq. (2). Equation (4) represents the whole amplitude distribution:

$$u(x,y) = \sum_{i=1}^{N} (H_i(x, y, z = 0)). \quad (4)$$

2. Ray-Tracing Method for CGH

In the field of CG rendering, the ray-tracing method is a method of simulating an image that is observed at a certain point by tracking a ray. By tracking the ray that reaches a certain point (such as the observer) in reverse, this method can express the object in the scene at that point. By doing so, it is possible to obtain the reflection of light on the surface of the object or the transparency and refraction of the object very well. Then, rendering is performed by coloring the corresponding pixel at the intersection point that is closest to the viewpoint [22,23]. In addition, since the path of the rays is computed pixel by pixel on the screen, the ray-tracing method can draw with a very high image quality. On the other hand, however, there is also a disadvantage that the amount of calculation is increased. In this method, the reflection and refraction of an object can be faithfully reproduced, but diffraction requires approximation and modeling. Although the fundamental principles of tracking the propagation path are common even if the objects are different, the calculation procedure differs for each. In CGHs, the ray-tracing method is also calculated as shown in Fig. 1. We omit the rays from the viewpoint at regular intervals, and the point where the ray intersects the object is the point light source. By applying this ray-tracing method to CGHs [24], the CGH rendering method using the ray-tracing method is able to express hidden surface removal, shading and shadowing, object refraction, etc.

B. Proposed System

In the previous section, we introduced the ray-tracing method for CGHs that can be used to display a real scene for CGHs. Since a number of works about the acuity of the human eye have been performed to show the minimum angle of resolution of the human eye due to the change of the angular distance away from the central gaze direction, we therefore used the representative result in our proposed method. Because of this result, we render the CGH reconstruction image into two areas: an inner area for the central gaze area and the outer area for the peripheral area. The inner area (fovea region within 5°) would be rendered in high resolution, and based on this result, the resolution of the outer area (based on our holographic device, we could display a reconstruction image only within 8°, so we chose a field of view from 5° to 8°) needs to be only half of the inner area. However, in the next experimental section, we still set the resolution of the outer area into several different levels to prove whether this will affect observing the reconstruction image.

1. Resolution Based on Radius of Fresnel Zone Plate

Since there is no need to render the outer area in high resolution, we can reduce the resolution of the outer area by expanding the angle of the ray. In our proposed method, the angle of the ray can be controlled freely, so we can expand the angle of the ray in the outer area, as shown in Fig. 2. However, if we expand only the angle of ray, when observing the reconstruction image, the continuous surfaces of the object would become discrete points, as shown in Fig. 3; the snowman and snowflake appear as continuous surfaces without the expansion of the angle of the ray, and appears as discrete points due to the expansion of the angle of the ray. To solve this problem, we need to fill these gaps between the discrete points.

A zone plate is a diffractive optical element that consists of several radially symmetric rings called zones. The zones alternate between opaque and transparent and are spaced so that light transmitted by the transparent zones constructively interferes at the desired focus, as shown in Fig. 4. In addition, a CGH is recorded by collecting the zone plate of all the point light sources. Based on Rayleigh theory, in CGHs, the resolution limit of the point light ω_{FZP} is determined by the radius r of the zone plate [25], defined as

$$\omega_{\text{FZP}} = C_\omega \cdot \lambda F, \quad (5)$$

where C_ω is a constant number, λ represents the wavelength of light, and the F number is the division of the distance z_r by the diameter of the hologram $2r$. Thus, we can replace the F with z_r and r, defined as

$$\omega_{\text{FZP}} = C_\omega \cdot \lambda \cdot \frac{|z_r|}{2r}. \quad (6)$$

Because of this equation, we can reduce the radius of the zone plate to make the point light larger and more blurred to fill the gaps between the discrete points of the object. The detail between the radius and resolution limit is shown in the experimental section.

2. Luminance Based on Radius of Fresnel Zone Plate

In the previous section, we introduced our method to reduce the radius of the Fresnel zone plate to make the point light larger and more blurred to fill the gap between the discrete points of the object. However, when we reduce the radius of the Fresnel zone plate, the luminance of the reconstructed point light would also become weak due to the reduction of the radius. The luminance L_R can be defined as

$$L_R = C_R \cdot \frac{1}{F^2}, \quad (7)$$

where C_R is the constant number. As we know, in a camera, the amount of luminance captured is proportional to the area of the
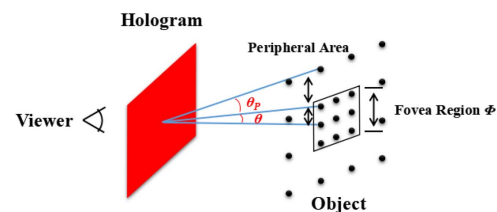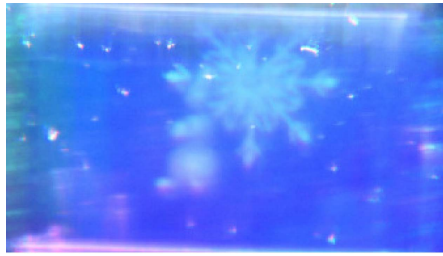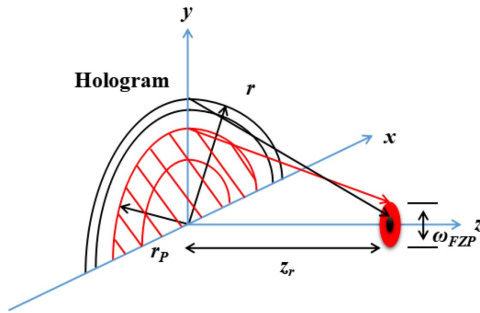

Fig. 2. Decrease of number of rays.

Continuous surfaces of snowman and snowflake   Discrete points of snowman and snowflake

Fig. 3.   Snowman and snowflake.

Fig. 4.   Reduction of radius.

aperture [26], in other words, it is inversely proportional to the square of the F number. Therefore, as in CGHs, we can replace F with r_P, which is the radius of the hologram and is defined as

$$L_R = C_R \cdot r_P^2. \tag{8}$$

Because of this equation, the luminance of the reconstructed point light is in proportion to the area of the Fresnel zone plate. Since we reduced the radius of the zone plate to make the point light larger and more blurred, the area became smaller, and the luminance of the reconstructed point light became weak. Thus, when generating a CGH, we need to correct the A_i, as shown in Eq. (2), to solve this problem. The details of the correction are shown in the experimental section.

3. Fast Calculation of CGH Based on Foveated Rendering

By applying foveated rendering with our proposed method, we can realize fast calculation of CGHs to reduce the cost of calculation. The high speed of our proposed method is mainly caused by the following two aspects: the reduction of the radius of the Fresnel zone plate, which reduced the resolution and is shown in Fig. 4, and the decrease of the number of rays due to the increase of the ray angle interval in the peripheral area, which is shown in Fig. 2. Also, the Eq. (6) could be written with

$$r = \frac{\lambda \cdot C_\omega}{2\theta}. \tag{9}$$

The non-foveated calculation of time complexity O is defined as

$$O\left(\frac{L^4 r^2}{\theta^2}\right), \tag{10}$$

which, because of Eq. (9), can be written with

$$O\left(\frac{L^4}{\theta^4}\right), \tag{11}$$

or written with

$$O(L^4 r^4), \tag{12}$$

where L represents the size of the hologram, θ represents the sampling interval of the fovea region, and r represents the radius of the zone plate in the fovea region. Since the calculation of time complexity decreases in proportion to the fourth power of the ray angle interval and the radius of zone plate, as shown in Eqs. (11) and (12), the reduction in calculation time by our method becomes very large due to both the effect of decreasing the number of point lights and the radius of the zone plate. The time complexity of foveated rendering calculation of fovea region O_F can be defined as

$$O_F\left(\frac{\Phi^4}{\theta^4}\right), \tag{13}$$

and the peripheral area O_P can be defined as

$$O_P\left(\frac{L^4 - \Phi^4}{\theta_P^4}\right), \tag{14}$$

where Φ represents the size of the fovea region, θ_P represents the sampling interval of the peripheral area, and r_P represents the radius of the zone plate in the peripheral area.

From Eqs. (13) and (14), by increasing the sampling interval, which means decreasing the number of rays, and decreasing the radius of the zone plate in the peripheral area, which reduces the reduction, we can get a fast CGH calculation in our proposed method.

4. EXPERIMENTS AND RESULTS

In this section, we are mainly talking about the experiments and results obtained by our proposed method. We conducted three different theoretical experiments to show the correctness and high speed of our proposed method, and one subjective experiment with 12 subjects to test whether the foveated rendering for CGHs is effective for viewers. All the experiments were based on the environment of a computer and holographic display [27], as shown in Tables 1 and 2, and Fig. 5.
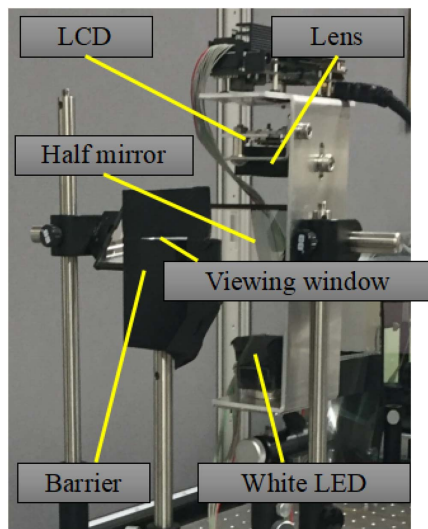
Table 1.   Parameters of Computer

| CPU	Intel Core i7-6700
OS	Windows 7 Professional 64 Bit
RAM	8.0 GB
Clock frequency	3.40 GHz
GPU	NVIDIA GeForce GTX TITAN

Table 2.   Parameters of Holographic Display

Pixel pitch of SLM	9.6 μm × 9.6 μm
Number of pixel	1280 × 768 pixels
Refresh rate of SLM	180 Hz
Wavelength of each color	red, 625 nm; green, 525 nm; blue, 465 nm

Fig. 5.   Holographic display.

A. Experiment for Resolution

In this experiment, we are mainly going to verify the relationship between the resolution and the radius of the Fresnel zone plate. From Eq. (6) we know that the resolution is in proportion to the radius, which means when the radius becomes smaller, the size of the point light becomes larger and more blurred.

To show whether the resolution is becoming lower, we generate a CGH, as shown in Fig. 6. In the middle of the image, we set several red rectangles with different gaps between each other, and the angle of the gap between the rectangle from right to left is from 0.025° to 0.2°. Since the minimum angle of resolution of our holographic display is 0.05°, we can see only the second gap between the rectangles. As a prediction, when we reduce the radius of the Fresnel zone plate, the point light would become larger, and the gap would be filled with the reducing of the resolution. The results are shown in Fig. 7, where we changed nothing but the radius. From the results, when the radius of the zone plate is becoming smaller, the gap is
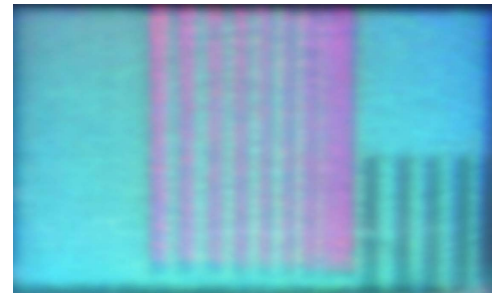
Fig. 6.   Reconstruction image without changing radius.

obviously filled until the red rectangles become a whole and cannot be distinguished from each other. These results verify that the resolution changes with different radius of the Fresnel zone plate correctly. The graph showing the proportion of the resolution and the proportion of radius compared with the non-foveated image is shown in Fig. 8, which matches Eq. (6).

B. Experiment for Luminance

In this experiment, we are going to prove the change between the luminance of point light and the area of the Fresnel zone plate. As shown in Eq. (8), the luminance became weak due to the reduction of the area.

Since it is not that easy to determinate the luminance directly, we are going to detect the average RGB value of the reconstruction image changing with the luminance. However, the RGB value is not changed with the luminance linearly, so we need to determinate the relationship between the RGB value and luminance first. As we know, for a camera, when the shutter speed doubles, the amount of incoming light would also double with no change of the other parameters of the camera. Therefore, we measured the RGB value by changing the shutter speed of the camera so that we could know the relationship between the RGB value and luminance. After that, we changed the radius of the Fresnel zone plate to 1/2, 1/3, and 1/4, which means the area of the Fresnel zone plate changed to 1/4, 1/9, and 1/16 compared with the non-foveated image. We measured the average RGB value of each reconstruction image and calculated the luminance proportion for the radius of the non-foveated image. The graph of the result is shown in Fig. 9. Because of the result, the luminance was changed with changing the area of Fresnel zone plate linearly. This verifies the luminance is changing with the area of the Fresnel zone plate correctly, which matches Eq. (8).

Because of this result, when we reduce the radius, we can correct the luminance of the reconstruction image to make sure the luminance of the peripheral area is the same as the fovea region. The corrected pattern of the CGH is shown in Fig. 10, as we can see that the zone plate in the peripheral area has become brighter than the zone plate in the fovea region, so that we can prove the correctness of the correction. The luminance of the Fresnel zone plate with reduced radius was corrected by making A_i in Eq. (2) inversely proportional to r_p^2. However, when we observed the reconstruction image, we still
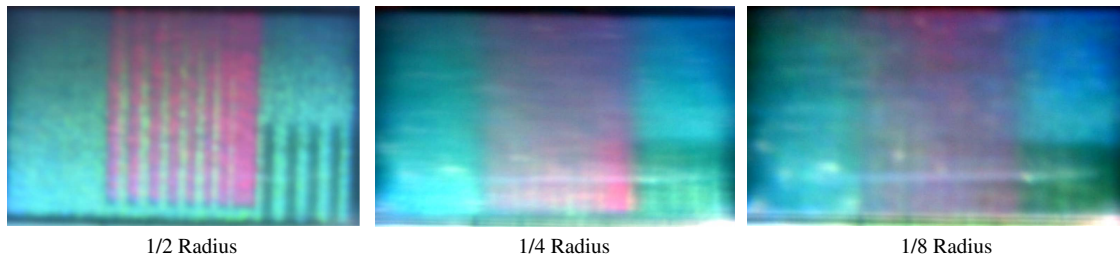
| 1/2 Radius | 1/4 Radius | 1/8 Radius |

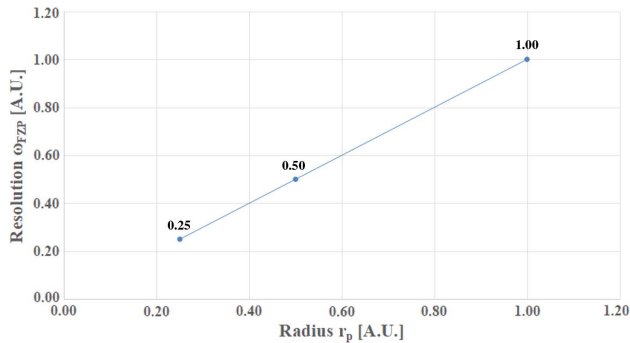**Fig. 7.** Reconstruction images with 1/2, 1/4, and 1/8 radius.

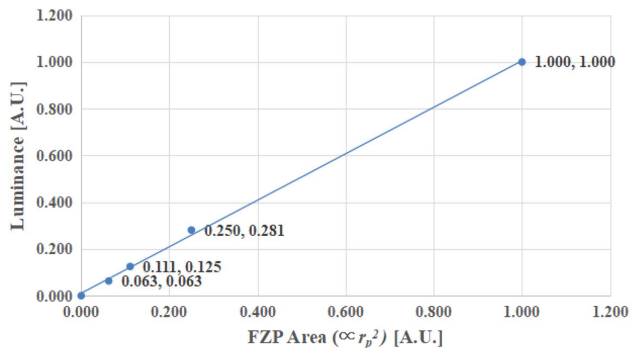**Fig. 8.** Proportion of resolution and radius compared with non-foveated image.

Fig. 9. Luminance changed with area of Fresnel zone plate.

felt the whole image was darker than the original non-foveated image. This is because of the reduction of the diffraction efficiency. Therefore, when we perform the subjective experiment, we have to adjust the luminance of the other reconstruction

images based on the darkest image to make sure the result is not affected.

C. Experiment for Calculation Time
Here, we are going to talk about the calculation time of our proposed method. The high speed of our proposed method is caused mainly by the following two aspects: the reduction of the radius of the Fresnel zone plate and the decrease of the number of rays due to the increase of the ray angle interval in the peripheral area. Figure 11 shows the result of the calculation time of wave propagation with the non-foveated image, a foveated image with 0.1° ray angle interval and 1/2 radius in the peripheral area, a foveated image with 0.2° ray angle interval and 1/4 radius in the peripheral area, and a foveated image with 0.3° ray angle interval and 1/6 radius in the peripheral area. The object we used is a checkerboard with 324 points and 162 faces. From the results, we got a 1.5 times higher calculation speed in the foveated image with 0.1° ray angle interval and 1/2 radius in the peripheral area compared with the non-foveated image. This result shows the high speed of our proposed method. Furthermore, if we have a wider field of view than 8° as our holographic display, we can get a higher calculation speed, as shown in Fig. 12. We conclude that our proposed method can improve the calculation speed by a factor of over 21 in the 30° field of view.

D. Subjective Experiment
In this experiment, we are going to test whether the foveated rendering for CGH is effective for viewers. We conducted a pair test after adjusting the luminance of other reconstruction images based on the darkest image with 12 subjects to evaluate the quality of the reconstruction image. We show the results as the average of all the subjects.

The pair test presented each user with pairs of three kinds of images. Each was shown for 2 s and was separated by a short black screen (for 1 s). The reference reconstruction image of the
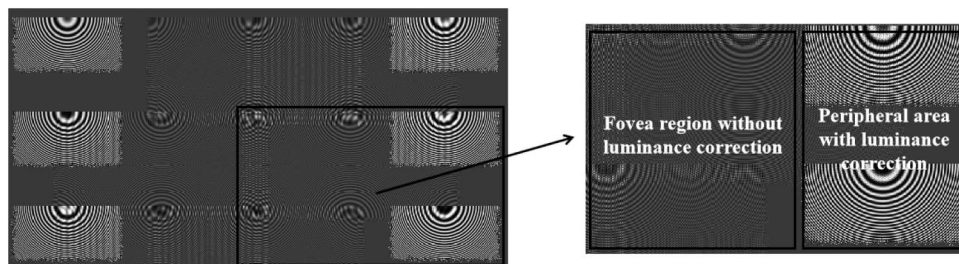

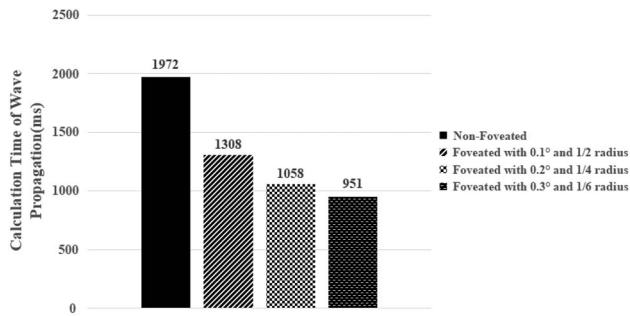**Fig. 10.** Luminance-corrected pattern of CGH.
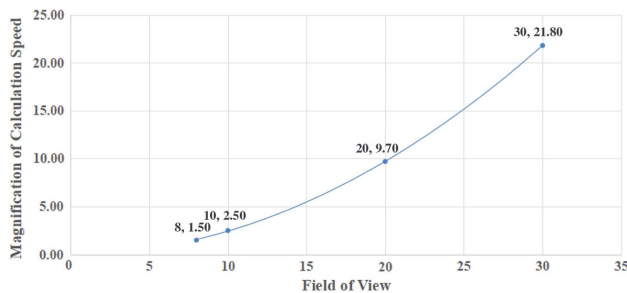
Fig. 11. Calculation time of each foveated quality.

Fig. 12. Calculation speed in wider field of view.

pair used non-foveated rendering with a ray angle interval of 0.05°; the other used foveated rendering at quality levels of $q = 3$ (high quality), 2 (medium quality), and 1 (low quality), which is ray angle intervals of 0.1°, 0.15°, and 0.2° with radii of

Table 3.   MOS Evaluation

5	Do not mind the difference
4	Not too mind the difference
3	Hard to say on both sides
2	A little mind the difference
1	Mind the difference

the zone plate of 1/2, 1/3, and 1/4 compared with the non-foveated rendering image at the peripheral area. The pair test at all quality levels in this range was presented twice in both orders (high quality to low quality, and low quality to high quality). After seeing each pair, users reported how they felt the quality changed compared with the non-foveated rendering image and evaluated the foveated rendering image with the mean opinion score (MOS) method, as shown in Table 3. Also, as the fovea region was rendered in the center of the image, users had to focus on the center of the image to evaluate the quality. The sample of reconstruction images is shown in Fig. 13.

Originally, we should use the resolution of 0.017°, as shown in α_0 of Eq. (1) at the fovea region and the resolution of 0.034° in high-quality foveated rendering. However, since the current holographic device cannot display resolution that high, we have to fit the resolution of the holographic display to perform the subjective experiments with 0.05° in the fovea region and 0.1° in the high-quality foveated rendering. Therefore, as a preliminary experiment, the subjects will still notice the difference even in high-quality foveated rendering. The evaluation results are shown in Fig. 14. These results indicate that even the resolution of the peripheral area is insufficient; we still got the

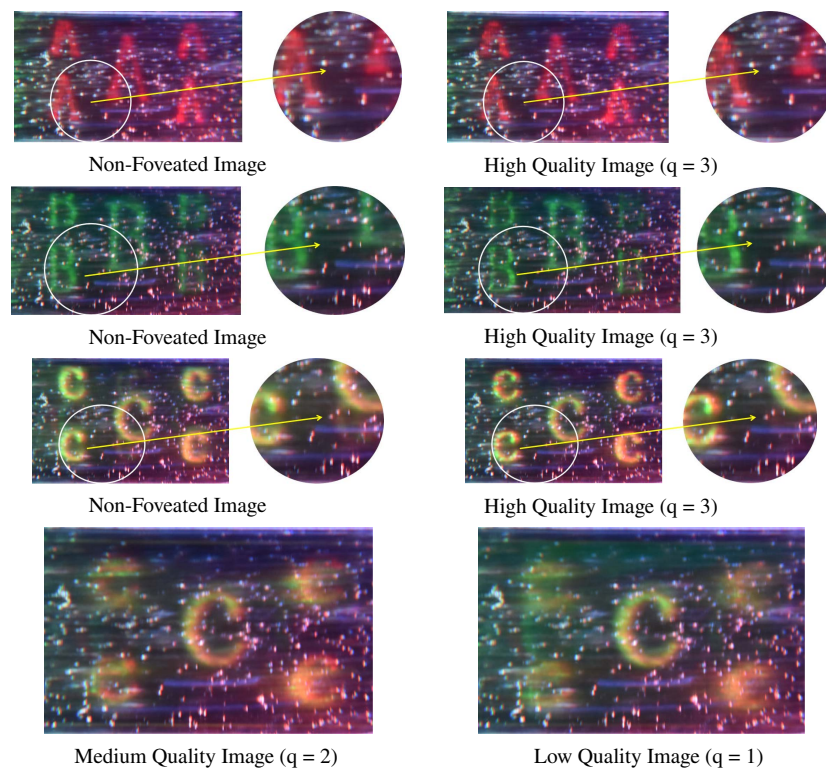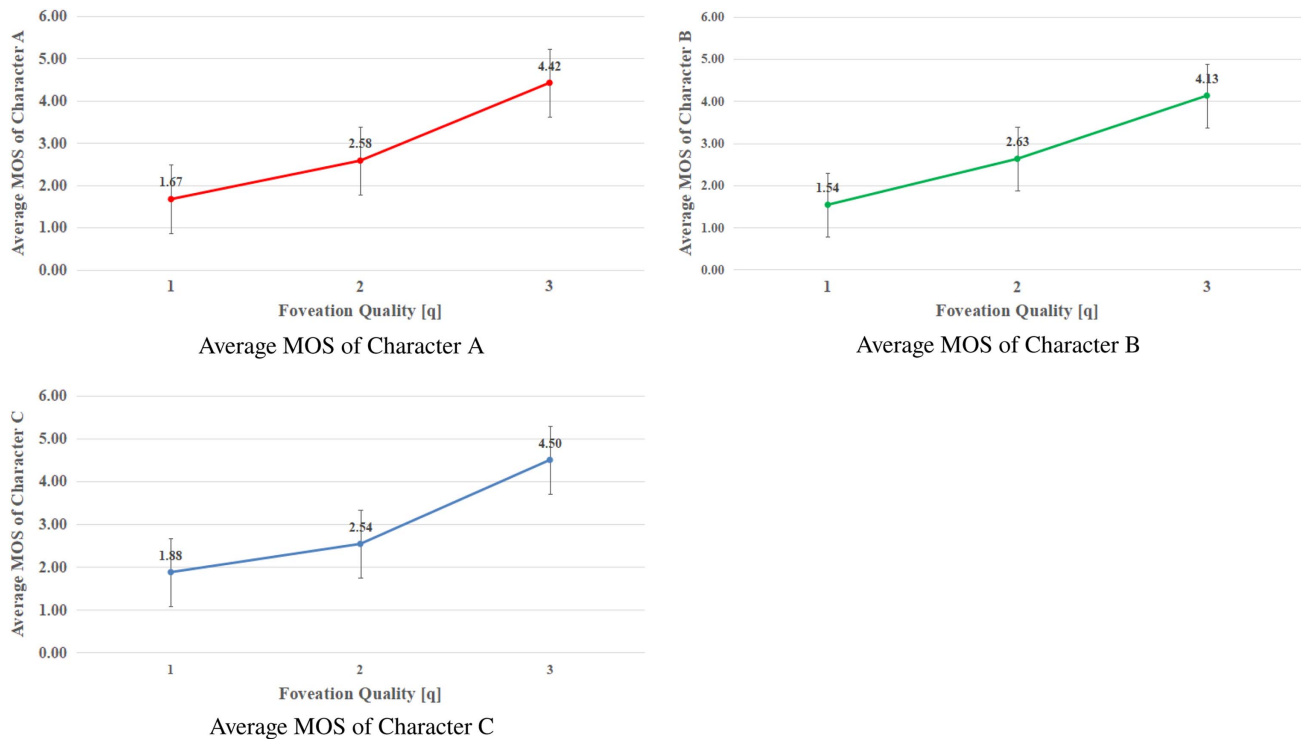
Non-Foveated Image

High Quality Image (q = 3)

Non-Foveated Image

High Quality Image (q = 3)

Non-Foveated Image

High Quality Image (q = 3)

Medium Quality Image (q = 2)

Low Quality Image (q = 1)

Fig. 13. Sample of reconstruction images.

Average MOS of Character A

Average MOS of Character B

Average MOS of Character C

Fig. 14.   Average MOS of characters A, B, and C.

evaluation of each kind of image in high quality all over 4, which means users almost did not know the quality difference between the non-foveated rendering image and the foveated rendering image. Also, as the quality become lower, the evaluation results became lower, which means users could feel the quality change as the resolution of the peripheral area became worse. In the future, we need to perform subjective experiments with a high-resolution device to confirm the correctness of our proposed method.

5. CONCLUSION

In this study, we proposed a method for CGH fast calculation with foveated rendering using an angle-changeable ray-tracing method, which is a new method for peripheral area rendering of CGH with reducing the radius of the zone plate and ray number to increase calculation speed. Our experiments show that by using foveated rendering, we can improve calculation speed in high foveated quality by a factor of 1.5 on current desktop displays compared with a conventional CGH rendering method. Furthermore, we can improve the calculation speed by a factor of over 21 in the 30° field of view. Also, by our subjective experiment, we concluded that even the current resolution of the holographic display is insufficient; there is still almost no influence for viewers to observe a CGH reconstruction image in high-quality foveated rendering. Though our system uses a general desktop display, its approach and experimental results can also be applied to a head-mounted display. In the future, we are mainly going to solve the problem of the low diffraction efficiency that made the reconstruction image darker than the original non-foveated image and perform subjective experiments with a high-resolution device to confirm the correctness of our proposed method.

REFERENCES

1. L. Zhang and J. T. Wa, "Stereoscopic image generation based on depth images for 3DTV," IEEE Trans. Broadcast. **51**, 191–199 (2005).
2. J. J. Laviola, "Bringing VR and spatial 3D interaction to the masses through video games," IEEE Comp. Graph. Appl. **28**, 10–15 (2008).
3. T. Shibata, "Head mounted display," Displays **23**, 57–64 (2014).
4. D. Gabor, "A new microscopic principle," Nature **161**, 777–778 (1948).
5. T. Yoneyama, E. Murakami, Y. Oguro, H. Kubo, K. Yamaguchi, and Y. Sakamoto, "Holographic head-mounted display with correct accommodation and vergence stimuli," Opt. Eng. **57**, 061619 (2018).
6. B. Guenter, M. Finch, S. Drucker, D. Tan, and J. Snyder, "Foveated 3D graphics," ACM Trans. Graph. **31**, 164 (2012).
7. *Understanding Foveated Rendering* (Sensics, 2016), pp. 57–64.
8. A. T. Duchowski, "A breadth-first survey of eye-tracking applications," Behav. Res. Methods Instrum. Comput. **34**, 455–470 (2002).
9. C. O'Sullivan, J. Dingliana, and S. Howlett, *The Mind's Eye: Cognitive and Applied Aspects of Eye Movement Research* (2002), pp. 555–571.
10. E. Reingold, L. C. Loschky, G. W. McConkie, and D. M. Stampe, "Gaze-contingent multiresolution displays: an integrative review," Hum. Factors **45**, 307–328 (2003).
11. A. T. Duchowski and A. Çöltekin, "Foveated gaze-contingent displays for peripheral LOD management, 3D visualization, and stereo imaging," ACM Trans. Multimedia Commun. Appl. **3**(4), 6 (2007).
12. P. Baudisch, D. Decarlo, A. T. Duchowski, and W. S. Geisler, "Focusing on the essential: considering attention in display design," Commun. ACM **46**, 60–66 (2003).
13. B. Watson, N. Walker, L. F. Hodges, and A. Worden, "Managing level of detail through peripheral degradation: effects on search

performance with a head-mounted display," ACM Trans. Comput. Hum. Interact. **4**, 323–346 (1997).

14. B. Watson, N. Walker, and L. F. Hodges, "Suprathreshold control of peripheral LOD," ACM Trans. Graph. **23**, 750–759 (2004).

15. H. Strasburger, I. Rentschler, and M. Jüttern, "Peripheral vision and pattern recognition: a review," J. Vis. **11**(5), 13 (2011).

16. S. Kazempourradi, B. Soner, E. Ulusoy, and H. Ürey, "Full-color foveated three-dimensional holographic near-to-eye display," in *International Symposium on Display Holography (ISDH)*, June 2018.

17. J. Hong, Y. Kim, S. Hong, C. Shin, and H. Kang, "Gaze contingent hologram synthesis for holographic head-mounted display," Proc. SPIE **9771**, 97710K (2016).

18. J. P. Waters, "Holographic image synthesis utilizing theoretical methods," Appl. Phys. Lett. **9**, 405–407 (1966).

19. D. J. DeBitetto, "Holographic panoramic stereograms synthesized from white light recordings," Appl. Opt. **8**, 1740–1741 (1969).

20. M. C. King, A. M. Noll, and D. H. Berry, "A new approach to computer-generated holography," Appl. Opt. **9**, 9471–9475 (1970).

21. K. Matsushima and S. Nakahara, "Extremely high-definition full-parallax computer-generated hologram created by the polygon-based method," Appl. Opt. **48**, H54–H63 (2009).

22. A. Appel, "Some techniques for machine rendering of solids," in *AFIPS Joint Computer Conference* (1968), pp. 37–45.

23. T. Whitted, "An improved illumination model for shaded display," Commun. ACM **23**, 343–349 (1980).

24. T. Ichikawa, T. Yoneyama, and Y. Sakamoto, "CGH calculation with the ray tracing method for the Fourier transform optical system," Opt. Express **21**, 32019–32031 (2013).

25. E. Moon, M. Kim, J. Roh, H. Kim, and J. Hahn, "Holographic head-mounted display with RGB light emitting diode light source," Opt. Express **22**, 6526–6534 (2014).

26. H. L. Gibson, *Close-Up Photography and Photomacrography*, 2nd combined ed., Vol. **2** of Photomacrography (Eastman Kodak, 1975).

27. T. Yoneyama, C. Yang, Y. Sakamoto, and F. Okuyama, "Eyepiece-type full-color electro-holographic display for binocular vision," Proc. SPIE **8644**, 864413 (2013).